Applied Catalysis B: Environmental 253 (2019) 88–95

Contents lists available at ScienceDirect

Applied Catalysis B: Environmental

journal homepage: www.elsevier.com/locate/apcatb

Immobilization of P450 BM3 monooxygenase on hollow nanosphere composite: Application for degradation of organic gases pollutants under solar radiation lamp

Gamal Awad[a], Elham Farouk Mohamed[b,*]

[a] Chemistry of Natural and Microbial Products Department, Pharmaceutical and Drug Industries Research Division, National Research Centre, 33 EL Bohouth St. Dokki, Giza, P.O.12622, Egypt

[b] Air Pollution Department, Environmental Research Division, National Research Centre, 33 EL Bohouth St. Dokki, Giza, P.O.12622, Egypt

ARTICLE INFO

Keywords:
P450 BM3 enzyme
Engineered *C. coli*
Immobilization
Hollow nanosphere
Air pollution
Remediation
Photonanobiocatalyst
Propanol
Sun light

ABSTRACT

Recently, nanoparticle-based immobilization of biocatalytic systems is getting interested in bioremediation efficiency. Therefore, hollow nanosphere particles of TiO_2 - Cu (< 50 nm) were used to immobilize P450 BM3 enzyme produced by engineered *E. coli* to create an effective novel material that can be significantly used for organic pollutants degradation under solar radiation conditions. Scanning Electron Microscope (SEM) and the evaluation of enzyme activity before and after immobilization step were used to confirm the successful immobilization process of enzyme on the surface of hollow nanosphere TiO_2 – Cu composite. The enzyme P450 BM3 was strongly immobilized on hollow nanosphere composite and its activity was doubled than that of the free enzyme produced by batch fermentation of engineered *E. coli*. Furthermore, the catalytic potential of P450 BM3 - hollow nanocomposite biocatalyst was examined for *in vitro* degradation of isopropanol as a model of organic gases pollutants under visible radiation. It was found that the degradation of isopropanol was high (95%) with enzyme- hollow nanosphere composite biocatalyst (5 mg) at an initial condition of pH (˜7.0), ambient temperature, and isopropanol concentration (20 mg/L). Control experiment indicated that P450 BM3 enzyme- hollow nanosphere composite biocatalyst was better than both the hollow nanosphere composite without enzyme and free enzyme. Therefore, the hollow nanocomposite TiO_2 – Cu seemed to enhance stability and activity of immobilized P450 BM3 enzyme over the free enzyme. Moreover, a combination of nanomaterial and enzyme is required for achieving biocompatibility and inert condition without denaturing the enzyme. Overall, TiO_2 -Cu hollow nanosphere composite is potential for large-scale P450 BM3 immobilization with improved properties and reuse. The results showed that the performance of nanobiocatalyst was successfully introduced via combined biocatalytic property of the enzyme and photocatalytic property of the hollow nanosphere composite. These were carried out for the first time in this paper. Therefore, this system is a potentially valid approach for air pollution remediation with a bright future in industrial applications as a new photonanobiocatalyst.

1. Introduction

Management the air pollution problem is a significant interest today, and it is increasing with each passing year and leading to grave and harmful effect to the earth. Numerous industries and human activities are responsible for this problem and high levels of dangerous pollutants like volatile organic compounds, CO, hydrocarbons, chlorofluorocarbons, and nitrogen oxides are noticed. In order to solve air and water pollution problems, several conventional methods have been used which include adsorption, thermal incineration, wet scrubbing ion exchange, photocatalytic oxidation, ozonation and botanical biofiltration [1–5]. Indeed, some studies on these methods showed that there are not able to effectively decompose several pollutants and may also cause the generation of hazardous secondary pollutants by inefficient degradation process [6–8]. Therefore, there is an urgent need to new technologies more efficient and economic to detect and correctly treat toxic environmental pollutants [9–12]. Biotechnology and biological catalysts procedures are developing an attracting elective approach to deal with the several hazardous environmental contaminants [13,14]. Among these methods, enzymatic processes have attracted significant

* Corresponding author.
E-mail addresses: awad_gamal7@yahoo.fr (G. Awad), elham_farouk0000@yahoo.com (E.F. Mohamed).

https://doi.org/10.1016/j.apcatb.2019.04.045
Received 9 March 2019; Received in revised form 11 April 2019; Accepted 15 April 2019
Available online 17 April 2019
0926-3373/

interest in the last few years to degrade different types of organic pollutants. Enzyme application process has been known as a promising alternative and environmentally friendly biotechnology for treating the pollutants present in air and water as compared to the conventional technologies [15–19]. They are used in the field of biodegradation, biosensors and bioremediation of different environmental pollutants due to their specific oxidation properties [20–24]. However, the disadvantages and limitations of enzymes using in different industrial application are their low operational stability, high price and short lifetime [25–27]. Therefore, the development of efficient enzymes applications technologies have strong stability and effectively overcome the drawbacks that restrict the free enzyme efficiency in the industrial application has become a bright topic in many domains. Immobilization of the enzyme on a suitable carrier is promising approach to overcome these limitations by improving the selectivity, stability of the enzyme towards acidity, high temperature, and the performance in organic solvents [28,29].

Furthermore, enzyme immobilization results in improving the possibility of the enzyme separation from the reaction mixture and reuse thus, decrease the cost of the process [30]. Different carriers have been used as supports for enzymes immobilization such as natural and synthetic polymer materials (alginate, cellulose, chitin) and inorganic supports like zeolites, alumina, and mesoporous silica [31–34]. Supporting materials with large surface area lead to obtaining good enzyme immobilization efficiency. Among these materials, nanoparticles represent very ideal carriers, due to their idealistic advantages including their specific surface area, mass transfer resistance, and effective enzyme loading which determines the line of biocatalysts efficiency [35–39]. Hollow nanospheres are other promising carriers for enzyme immobilization in this study. They have large internal space thus, allow both the external and inner surfaces of the catalyst to contact with the reactants thus increase its catalytic activity, and may favor the harvesting of exciting visible light due to multiple scattering within the interior cavity and can effectively overcome the problem of electron − hole separation, and control the retention time of the photocatalyst, which make them promising applications in various fields [40]. Moreover, the combination of Pt doping and TiO_2 hollow structure has developed as a practical procedure for improving strong visible light absorption, great charge separation, and high surface area thus facilitating the enzyme immobilization and increasing its activity.

Recently, several immobilized enzymes in particular laccases, peroxidases, and dioxygenases have been applied in many advanced biotechnologies [41–43].

Cytochrome P450 s are a variety of enzymes having a particular ability in catalyzing the oxidation of different types of substrates such as drugs, hydrocarbons, xenobiotics, fatty acids, and aromatic compounds. As an important member of this family, P450 BM3 from *Bacillus megaterium* is a soluble enzyme that consists of both monooxygenase and reductase domains on a single polypeptide chain [44]. The later makes this protein a self-sufficient biocatalyst and a good model to study the catalytic behavior of P450 s. The enzyme P450 BM3 inserts a single oxygen atom from molecular oxygen into an organic substrate while the other one was reduced to a water molecule. For this selective oxidation process, P450BM3 requires O_2 and a continuous supply of electrons usually from cofactors such as nicotinamide adenine dinucleotide phosphate (NADPH). Because of enzyme low stability and continuous supply of an expensive cofactor, NADPH, it is not broadly used in industry. Enzyme immobilization on / onto / in different supports has been applied in several biotransformation processes to enhance the enzyme stability and reusability. However, there are only a few reports on the immobilization of P450 s BM3 [45]. For example, King and coworkers [46] reported successful immobilization of cytochrome P450 in both calcium alginate and CNBr activated sepharose for benzopyrene hydroxylation. Owing to the increasing attention in the biotechnological applications of oxidoreductases, it seems that it is very important and necessary to immobilize such enzymes on other types of nanocarriers to create stable systems and to increase the application value of these enzymes.

This work aims to immobilize for the first time P450BM3 enzyme produced by engineered *Escherichia coli* BL21 on hollow nanosphere TiO_2 - Cu particles, to characterize the novel prepared enzyme-nano composite system by SEM analysis, to apply the prepared bionanocatalyst for the degradation of isopropanol as a model for organic gases pollutants under a solar radiation lamp at ambient conditions and finally to compare the results obtained with that of both free P450BM3 enzyme and nanocomposite free enzyme. This study presents for the first time a new bionanocatalyst based on P450BM3 enzyme operated with economic source of oxygen (H_2O_2) and continues supply of electrons derived from TiO_2-Cu hollow nanosphere when exposed to solar radiation lamp during the application that is a potentially valid approach for environmental pollution remediation with a bright future in many industrial fields.

2. Experimental

2.1. Materials

The cytochrome P450BM3 from *Bacillus megaterium* was optimized and expressed in *E. coli*. The histidine tag containing imidazole groups was added to the enzyme for purification and immobilization uses. All chemicals used were of analytical grade. Sucrose, titanium butoxide (TB), benzyl alcohol (BA), oleylamine (OM), benzyl ether, tetraethylammonium hydroxide (TEAOH), polyethyleneimine (PEI), ammonium hydroxide, and tetrachloroauric (III) acid were purchased from Sigma Aldrich, Canada. All of the reagents were used without further purification.

The yeast extract, tryptone, Ampicillin, KH_2PO_4, K_2HPO_4, Glycerol, $FeCl_3$, formaldehyde (37%), H_2O_2 (50%), sodium dithionite (85%) and IPTG (isopropyl-β-D-thiogalactoside) were purchased from Fisher Scientific Co. (Ottawa, Ontario, Canada).

2.2. Synthesis of hollow nano-supporting materials

2.2.1. Synthesis of carbon colloidal spheres

Typically, 32 g sucrose was dissolved in 160 mL de-ionized water which was then heated in a Teflon-lined autoclave at 160 °C for 6 h. Afterwards, the solid product was collected by centrifugation at 6000 rpm for 10 min, washed several times with water and ethanol, and dried overnight at 80 °C.

2.2.2. Synthesis of titanate nanodisks (TNDs)

Water-soluble TNDs was synthesized, briefly, 2 g of TB, 12 g of OM, 12 g of BA, and 30 g of benzyl ether were added to a 100 mL round-bottom flask. The reaction mixture was heated to 190 °C at the heating rate 5 °C/min under nitrogen flow. After 20 h, the reaction was cooled to room temperature. After excess addition of absolute ethanol, the TNDs were recovered and were subjected to three cycles of dispersion in toluene and re-precipitated with ethanol. Then, the synthesized TNDs were treated with a mixture of TEAOH (15 mmol), ethanol (15 mL), and de-ionized water (15 mL). The mixture was stirred overnight at room temperature followed by adding of acetone to obtain TNDs precipitate. Afterwards, the precipitate was washed several times with acetone and finally dispersed in 100 mL of de-ionized water.

2.2.3. Synthesis of carbon colloidal spheres/TNDs-Cu

As-prepared carbon colloidal spheres were coated with TNDs using a layer-by-layer deposition technique. The carbon colloidal spheres (2 g) was dispersed in 50 mL of de-ionized water containing 0.3 g PEI and stirred for 1 h to ensure the saturated adsorption of PEI on the surface of the carbon spheres. Excess PEI was removed by centrifugation before being subjected to 50 mL of H_2O containing 50 mg TNDs under stirring. The electrostatic force between the negatively charged

TNDs and positively charged PEI on the surface of carbon spheres forms a layer of TNDs on the surface of carbon spheres. The synthesized material was then recovered by centrifugation and washing. The above procedure was repeated for seven cycles to obtain the carbon colloidal spheres/TNDs. Then, as-prepared carbon colloidal spheres/TNDs were re-dispersed in 50 mL solution of 15 mM Cu $(NO_3)_2$. The resulting mixture was stirred for 1 h to ensure the adsorption of Cu on the carbon colloidal spheres/TNDs. After that, the precipitate was collected by centrifugation, dried at 70 °C overnight and calcined at 550 °C for 3 h to obtain hollow nanosphere /TiO_2-Cu.

2.3. Enzyme preparation

2.3.1. Heat shock protocol for plasmid production

Firstly, thaw cells (*E. coli* B121) on ice and add plasmid DNA containing the enzyme from *Bacillus megaterium* (0.5–1 µl) to microtubes (100 µl of cells) as soon as ice disappears then incubate cells on ice 30 min. Secondly, transfer microtubes to water bath at 42 °C for 45 s to 1 min and then add 500 µl Ampicillin antibiotic free Lysogeny broth (LB) medium to each microtube and incubate again at 37 °C for 1 h in the water bath. Finally, plate on selective agar plate Ampicillin for pET15B (1 mg/mL) and incubate at 37C° for 24 h in the incubator (Thermo Scientific).

2.3.2. Medium and pET15B culture conditions

A colony strain was grown on LB medium containing 1 µg/mL Ampicillin overnight at 37 °C in tube (50 mL). Aliquots (2%) of the cell culture from the tube were transferred to 100 mL Terrific Broth (TB) medium supplemented with 1 µg/mL Ampicillin in a 250 mL flask. The TB medium composed of (per liter distilled water): 12 g Tryptone; 24 yeast extract; 0.4% glycerol; 2.31 g KH_2PO_4 and 12.54 g K_2HPO_4, the pH was adjusted to 7.2. The shaking flask was incubated at 215 rpm/min and 37 °C. After reaching an optical density at 600 nm (OD_{600}) of 0.3, P450 BM3 enzyme expression was induced by adding 0.5 mmol/L IPTG for 7 h. Withdrawals were taken through the period of intervals of 0, 2, 4, 6 and 7 h. *E. coli* cells containing P450 BM3 were optimized and harvested. The most important influential parameters were selected by studying different concentrations of certain parameters as glycerol, $FeCl_3$ and trace elements for P450-BM3 enzyme production. For enzyme preparation, the cells were broken up under ice-cooling with Sonicator (output level 200 W, 3 × 15 s duty cycles of 20% each). The suspension was centrifuged for 10 min at 10,000 rpm at 4 °C. The crude extracts were used directly for the activity assay.

2.4. Enzyme production and purification

The enzyme was produced and purified according to previously modified methods [45]. After 7 h of induction, 20 mL cells of culture broth were harvested by centrifugation and washed twice with 50 mM Tris − HCl (pH 8.5) and the pellet was suspended in 5 mL of 50 mM sodium phosphate buffer (pH 7.0, 500 mM NaCl, 10 mM imidazole), and ultrasonicated on ice at 20 MHz, 30% amplitude, 3 cycles (30 s per cycle). After that, the samples were centrifuged at 10,000 g for 15 min (4 °C). The supernatant was introduced onto a 2.0 mL Ni affinity column equilibrated with 50 mM sodium phosphate buffer (pH 8.0, 500 mM NaCl, and 10 mM imidazole). After 30 min, the column was washed with 20 ml of the buffer containing 20 mM imidazole. The protein was eluted with 200 mM imidazole and dialyzed in 50 mM Tris − HCl buffer for 24 h. After dialysis, the enzyme activity and protein concentration of the purified P450 BM3 was determined.

2.5. Immobilization of P450 BM3 enzyme on holonanosphere

Immobilization of P450 BM3 enzyme on hollow nanosphere TiO_2-Cu was carried out by physical route i.e. adsorption (a non-covalent and reversible process). The previous synthesized hollow TiO_2-Cu nanoparticles (5 mg) were added to 200 µL of purified P450 BM3 freshly prepared in 0.1 M citrate-phosphate buffer (pH 5.0) and the mixture is gently shaken for 1 h at 160 rpm at room temperature, as adsorption equilibrium is achieved after 30 min of incubation. For a control, 200 µL of free enzyme was used. The samples were subsequently centrifuged for 5 min, and the supernatants were removed. Three washes with 1 mL of buffer (0.1 M, pH 7.0) were performed to remove unbound enzyme. After immobilization, solution was filtered out, and dried at ambient temperature. The activity of immobilized enzyme was determined with the same procedure used in free enzyme. The produced bionanocatalyst was characterized using SEM technique and then its oxidation performance was investigated using 20 µl isopropanol as a model of organic pollutant.

The immobilization of the P450 BM3 enzyme on the synthesized nanoparticles can take place through coordinating bonds between Cu^{2+} in the hollow nanosphere TiO_2-Cu surface and imidazole group of the enzyme. Furthermore, to cross-link the adsorbed enzyme on hollow nanosphere TiO_2-Cu surface, formaldehyde (0.5%, v / v) was added to activate the holonanoparticles. In 1 mL of phosphate buffer solution (PBS, 25 mM, pH7), formaldehyde was added to 5 mg hollow nanosphere TiO_2-Cu carrying 1 nmol of enzyme. The mixture was incubated at 4 °C, 25 rpm, for 2 h. Then, particles were separated and washed three times with PBS to remove the remaining formaldehyde. The cross linked-adsorbed enzymes were dispersed in the buffer and stored at 4 °C for further use.

2.6. Assay of P450 BM3

The method of Omura and Satu [47] was used to evaluate the enzyme concentration. A volume of enzyme solution was taken (1.2 mL) and put it in a cuvette (1 cm cell) in spectrophotometer (GYNESYS, Thermo Scientific, USA). Place the two cuvettes in the spectrophotometer and record a blank or baseline between 400 and 500 nm. Bubbles of CO (60–80) were bubbled into the enzyme solution. Sodium dithionite ($Na_2S_2O_4$, 1 mg) or the tip of a spatula was added to the enzyme solution saturated with CO. Pippet up and down and read data on the spectrophotometer until the value at 450 nm stops increasing. Record the highest value for 450 nm and also the values at 420 nm and 490 nm if those are positive. Use the formula of Guengerich and coworkers [48] to calculate the cytochrome P450 BM3 concentration.

Samples were taken before and after enzyme immobilization. The quantity of adsorbed enzyme was then calculated by the difference between the initial amount of enzyme before and the sum of the remaining and washed enzyme in the supernatant after immobilization. Prior to the experiment, pilot test using NADPH (100µM) as substrate was evaluated to determine the storage stability of immobilized system.

2.7. Photocatalytic activity of P450 BM3-holonanocatalyst

To evaluate the catalytic activity of P450 BM3-holonanocatalyst, isopropanol was used as the substrate under solar radiation lamp and then measure the concentration of generated CO_2. The photocatalytic decomposition of isopropanol was carried out in a top-irradiated reactor at ambient temperature and pressure using immobilized enzyme (1 nmol) on hollow nanosphere TiO_2-Cu, immobilized enzyme with 40 µl H_2O_2 (0.3 mL/L) as well as free enzyme (control). In a typical photocatalytic experiment 20 mg of the nanobiocatalyst, the optimum amount of the catalyst for this photocatalytic reactor system, was dispersed in the reaction cell. The reaction cell was then evacuated, and filled with fresh synthetic air. Then, a certain amount of isopropanol solution (20 µl) was injected into the reactor. Prior to light irradiation, the reaction cell was kept in the dark for four hours to ensure that an adsorption–desorption equilibrium of the reactant was established on the surface of the nanobiocatalyst. Then, the reactor cell was illuminated with visible light ($\lambda \geq 420$ nm) through au UV cut-off filter from a solar simulator 150-W Xe lamp, for 3 h. The amount of CO_2 gas

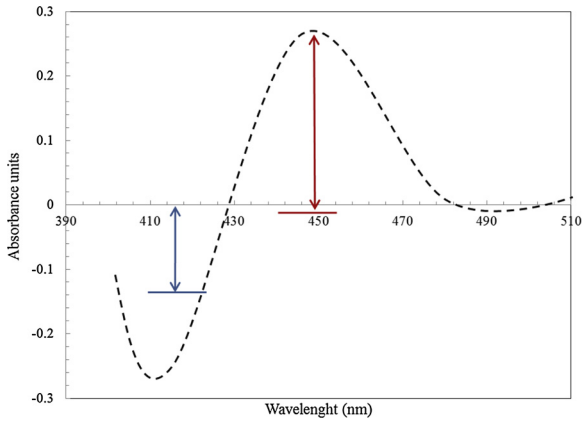

Fig. 1. Typical CO difference spectrum of P450 BM3 activity assay showing the maximal absorbance at 450 nm.

generated during the reaction was analyzed using a gas chromatograph (Agilent 7820 A) equipped with a thermal conductivity detector (TCD) with carboxen-1010 capillary column and He as the gas carrier.

3. Results & discussion

3.1. Determination of P450 BM3 enzyme assay

The enzyme P450 BM3 concentration was determined by the method reported by Omura and Satu [47]. The enzyme quantity was determined by applying the Beer – Lambert equation. The carbon monoxide difference spectra for P450 BM3 showed absorption maxima at 450 nm

(Fig. 1). When the size of the peak near 450 nm has stopped increasing, terminate the analysis. To begin the calculations, read the absorbance at 450, 490 and 420 nm. To calculate the concentration of the enzyme immobilized on the nanosphere particles, the concentration before and after immobilization was carried out. From results, the immobilized P450 BM3 enzyme was found to be 37.9 mg enzyme/g support. The later was achieved by enhancing the initial P450 BM3 concentration to 2923 nM (32.5% efficiency of immobilization). Türkmen and coworkers [49] cited 40.1 mg / g cytochrome c immobilized on magnetic/Cu^{2+} composite. Moreover, for the stability of the system it was found that the P450 BM3 enzyme immobilized on Pt/TiO_2-Cu hollow nanosphere was still active toward the NADPH after almost 35 days. However the free enzyme lost its activity toward the substrate after 7 days.

3.2. Immobilization of the crude enzyme on hollow nanoparticles

Crude enzyme P450 BM3 was immobilized on synthesized hollow TiO_2-Cu nanoparticles by physical route i.e. adsorption (a non-covalent and reversible process).

The presence of Cu^{2+} in the synthesized hollow nanosphere TiO_2-Cu surface can bind with the imidazole group of histidine on the enzyme through coordinating bonds leading to immobilize the P450 BM3 enzyme on the synthesized hollow nanoparticles. Furthermore, the addition of formaldehyde leads to cross-link the adsorbed enzyme on hollow nanosphere TiO_2-Cu surface, to activate the nanoparticles (Fig. 2).

Divalent transitional metal ions such as Ni^{2+}, Zn^{2+}, Co^{2+}, and Cu^{2+} can interact with the thiol group of cysteine, the indole group of tryptophan, or the imidazole group of histidine [50], for example, Cu^{2+} - magnetic nanoparticles have been successfully used to adsorb cytochrome c from its solution. Although the enzymes immobilized by metal affinity are often more active, because of the mild immobilization conditions, enzyme cross-linking is recommended to reduce the enzyme leakage [51].

SEM analysis was performed in order to investigate morphology, orientation and elemental composition of particles before and after immobilization. Results reveal the changes in the morphology of the particles before and after immobilization as shown in Fig. 3. As demonstrated in Fig. 3a, most nanoparticle samples are quite uniform nanospheres structure at the nano scale average < 100 nm. After calcination at 680 °C, the hollow structure was formed due to the combustion of the carbon colloidal spheres. As seen also in Fig. 3a, some broken particles and spheres have typical hollow interior structure were observed after calcination, clearly indicate the presence of the hollow nanospheres. The nitrogen adsorption –desorption isotherm data indicate that the surface area of hollow TiO_2-Cu nanoparticles is about 80 m^2/g. By comparison of features in Fig. 3a and b, it could be observed that there is a slight change in morphology and increased particle size to 200 −300 nm, that might be due to the formation of coordinating bonds between Cu^{2+} and enzyme function groups by metal affinity adsorption [52]. The change in particles morphology clearly revealed the successful immobilization of the enzyme on nanomaterials with stronger absorption and high enzyme loading. In particulate, the nano-scale and surface properties provided the suitable characteristics for enzyme immobilization [53]. Nano particles of immobilized sample were formed with average size below 50 nm.

Elemental mapping by energy-dispersive X-ray microscopy (EDX) from SEM analysis of the immobilized P450 BM3 enzyme on nanoparticles was clearly confirmed the homogeneous distribution of Ti, O and Cu, as depicted in Fig. 3c. The homogeneous distribution of these elements indicates efficient doping of different cations (Cu and Pt) into the TiO_2 lattice without a phase separation. In this approach, using carbon colloidal spheres with a high density of OH groups on the surface facilitated the adsorption of Cu^{2+} and Pt^{3+} cations, which resulted in a successful immobilization of P450 BM3 enzyme onto the hollow nanosphere.

The morphology of the immobilized P450 BM3 enzyme on hollow nanoparticles was further characterized by transmission electron microscopy (TEM) (Fig. 3d). Hollow nanospheres of 1 μm in average diameter were observed.

The X-ray diffraction patterns (XRD) of Pt/TiO_2-Cu hollow nanosphere and immobilized P450 BM3 enzyme on Pt/TiO_2-Cu hollow nanosphere are shown in Fig. 4a and b, respectively. It's clear from the figure that the X-ray diffraction patterns are mostly identical for the two samples, where the enzyme immobilization on the surface of nanoparticles did not lead to a phase change. The X-ray diffraction patterns indicates the presence of TiO_2 and Cu in the nanomaterial; no XRD peak characteristic of Pt was detected, this could be due to the small size of the Pt NPs (< 5 nm). Fig. 4a and b exhibit diffraction peaks at 2θ values of ca. 25.38°, 37.82°, 48.18° and 54.4° indicating that most TiO_2 in the prepared samples were anatase crystal structure. Furthermore, no impurity diffraction peaks were detected, indicating a pure phase of synthesized Pt/TiO_2-Cu hollow nanosphere.

3.3. Estimation of the catalytic efficiency of the immobilized enzyme /TiO2-Cu hollow nanosphere catalyst

The catalytic activity of the immobilized P450 BM3 enzyme on hollow nanosphere TiO_2-Cu was investigated using isopropanol gas as a model of volatile organic pollutants. To simulate the degree of the biodegradation activity, three experiments were separately designed and compared as follows: Free P450 BM3 enzyme, H_2O_2 /free P450 BM3 enzyme and finally H_2O_2/ P450 BM3 enzyme immobilized on TiO_2-Cu hollow nanosphere were used for isopropanol degradation and the concentration of the generated CO_2 gas was measured as end product of isopropanol biodegradation under visible light ($\lambda \geq 420$ nm) through au UV cut-off filter from a solar simulator 150-W Xe lamp. Results revealed that within 60 min, just a small amount of CO_2 (0.5 μmol) was released from isopropanol decomposition under visible

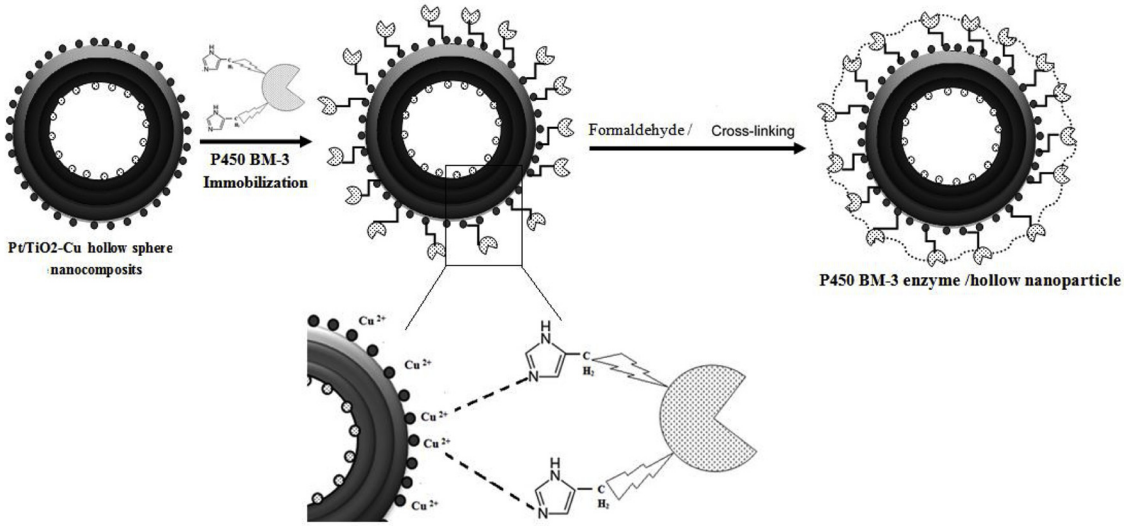

Fig. 2. Schematic illustration of the immobilization mechanism of the P450 BM3 enzyme on the hollow nanosphere Pt/TiO_2–Cu photonanocatalyst.

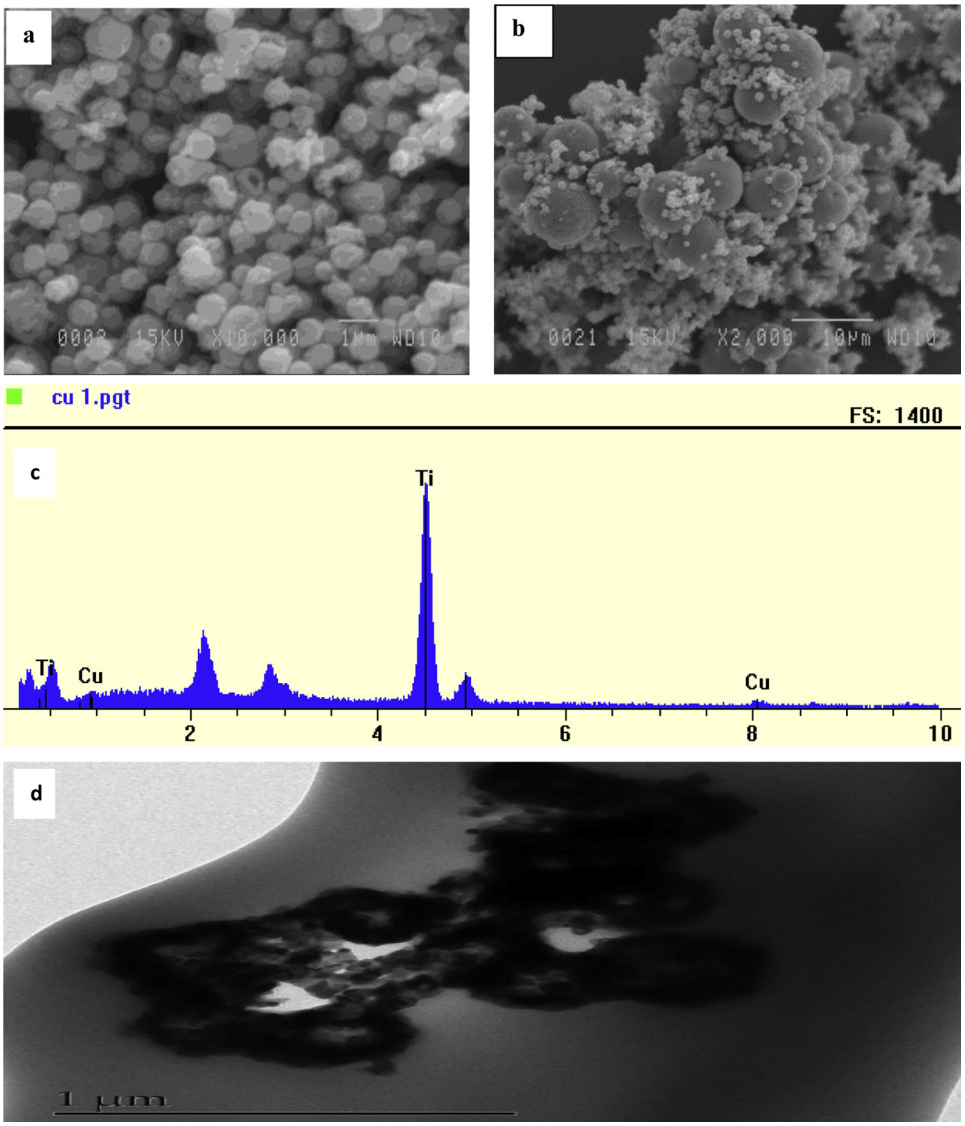

Fig. 3. SEM images of before (a) Pt/TiO_2-Cu hollow nanosphere composite and after immobilization (b) P450 BM3 enzyme immobilized on Pt/TiO_2-Cu hollow nanosphere, (c) EDX analysis and (d) TEM of the immobilized P450 BM3 enzyme on Pt/TiO_2-Cu hollow nanosphere.

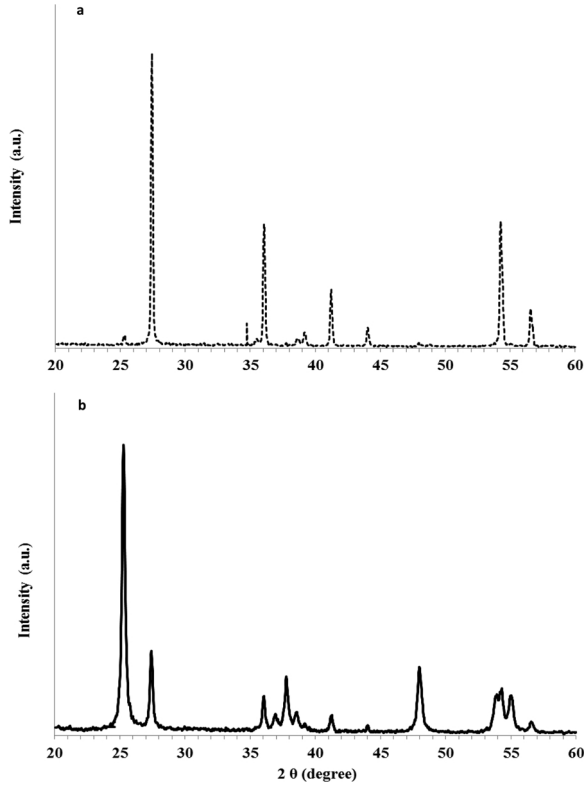

Fig. 4. The X-ray diffraction patterns of Pt/TiO_2-Cu hollow nanosphere (a) and immobilized P450 BM3 enzyme onto Pt/TiO_2-Cu hollow nanosphere (b).

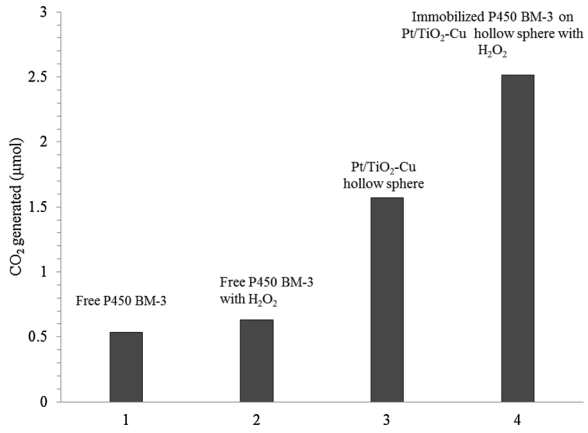

Fig. 5. The catalytic efficiency of the immobilized P450 BM3 monooxygenase enzyme on Pt/TiO_2-Cu hollow nanosphere under solar radiation lamp (λ ≥ 420 nm, 150-W) with and without H_2O_2 for the isopropanol degradation as volatile organic compound (CO_2 generated, µmol).

radiation by using P450 BM3 enzyme due to the smaller surface of free enzyme exposed to the reaction as compared to that of immobilized enzyme onto the nanoparticles. James and Elizabeth [54] reported also that the ability of P450 enzymes to oxidize and contribute to the degradation of persistent organic pollutants (POPs) is well known. P450 activities have been identified in the degradation of polycyclic aromatic hydrocarbons (PAHs) and polychlorinated biphenyls (PCBs). As depicted in Fig. 5, the presence of H_2O_2 has been slightly improved the photocatalytic activity of the free enzyme. As seen in Fig. 5, a very high catalytic activity of the P450 BM3 enzyme immobilized on TiO_2-Cu hollow nanosphere for the degradation of isopropanol gas was observed under visible light where the CO_2 concentration is about 5 times higher than that of the free P450 BM3 enzyme and also almost 67% more over the use of hollow nanosphere only.

Under optimized conditions, the photocatalytic degradation capacity of isopropanol was observed to be: immobilized P450 BM3 enzyme on TiO_2-Cu hollow nanosphere/H_2O_2 > TiO_2-Cu hollow nanosphere > free P450 BM3 enzyme/H_2O_2 > free P450 BM3 enzyme. Many previous studies [45,55] reported that the enzymes immobilized on nanoparticles show catalytic activities comparatively better than that of the unbound enzymes. The immobilized P450 BM3 enzyme/TiO_2-Cu hollow nanosphere system showed a synergetic effect of biocatalytic and photocatalytic degradation approaches [56,57]. The support TiO_2-Cu hollow nanosphere is able to generate electron-hole pair upon visible light illumination (˜solar radiation). The interaction of these electron-hole pairs with active species OH• (H_2O_2) resulted in isopropanol degradation. This gives two conditions required to function the P450 BM3 monooxygenase enzyme which are electron supply from TiO_2-Cu hollow nanosphere photocatalyst and oxygen supply from commercial H_2O_2.

The possible degradation mechanism of isopropanol by immobilized P450 BM-3 enzyme can be explained on the basis of hypothesis that isopropanol is firstly adsorbed on the surface of immobilized P450 BM-3 monooxygenase, followed by degradation process which involved both photodegradation by electron hole pairs generated by Pt/TiO_2-Cu hollow nanoparticles as well as biodegradation by the enzyme (Fig. 6). Under visible radiation, the photodegradation process resulted in formation of intermediates products which then adsorbed on the immobilized monooxygenase enzyme where the biodegradation of intermediates takes then place. The enzyme inserts a single oxygen atom from molecular oxygen (H_2O_2) into these organic intermediates to degrade them to CO_2 and H_2O while the other one was reduced to a water molecule. The generation of CO_2 is then evaluated and used as an indicator for the catalytic efficiency of the nanobiocatalyst. Overall, the combination of hollow nanosphere (photo-degradation) and monooxygenase enzyme (biodegradation) leads to complete mineralization of isopropanol.

3.4. Effect of the contact time

Comparative study was conducted to investigate the effect of contact time on the bio-photo degradation performance of both the immobilized P450 BM-3 enzyme on Pt/TiO_2-Cu hollow nanosphere and free P450 BM-3 enzyme in the presence of H_2O_2 as a source of oxygen. Fig. 7 revealed that by increasing the reaction time, the degradation of

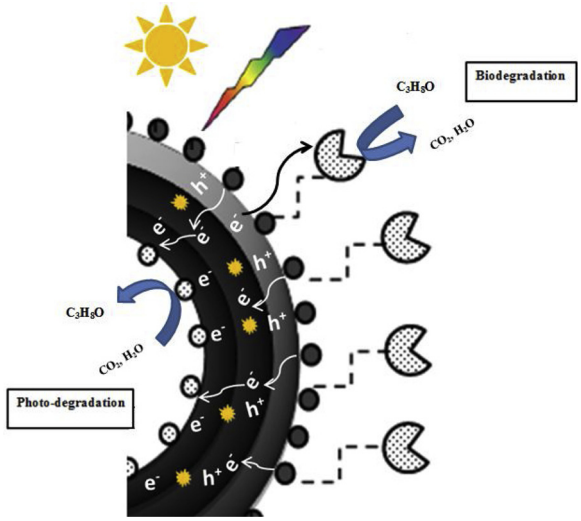

Fig. 6. Schematic illustration of the catalytic mechanism of the immobilized P450 BM-3 on Pt/TiO_2-Cu hollow nanosphere bionanocatalyst under solar radiation lamp (λ ≥ 420 nm, 150-W).

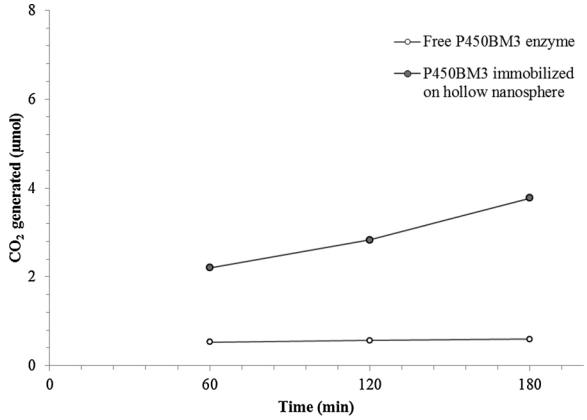

Fig. 7. Effect of contact time on the catalytic activity of free P450 BM-3 enzyme with H_2O_2 (open symbol) and P450 BM-3 enzyme immobilized on Pt/TiO_2-Cu hollow nanosphere with H_2O_2 (closed symbol).

isopropanol with the immobilized enzyme on nanosphere is greatly higher than that obtained with the free enzyme (control). During the first 60 min, free enzyme could be able to degrade the isopropanol due to the availability of active site at the beginning of the reaction but with increasing the exposure time no change was achieved. The performance was completely different and significant with the immobilized enzyme, where the combination of hollow nanosphere with the monooxygenase enzyme strongly enhances both the stability and activity of the enzyme [58]. Moreover, the combination of nanoparticles with enzyme provided a biocompatible and inert environment and also avoided direct exposure of metals or their oxides [59].

3.5. Analysis of operating costs

In this section a preliminary analysis of operating cost related to the use of P450 BM3 enzyme immobilized on Pt/TiO_2-Cu hollow nanosphere and compared to the free enzyme for the removal of VOCs is conducted. As seen in Fig. 5, the maximum isopropanol degradation using P450 BM3 enzyme immobilized on Pt/TiO_2-Cu hollow nanosphere is almost 5 times higher than that of the free P450 BM3 enzyme under the same condition. This means that free P450 BM3 enzyme required a 5-fold mass value in order to have an equivalent catalytic activity of P450 BM3 enzyme immobilized on Pt/TiO_2-Cu hollow nanosphere. Dong and co-workers [60] reported that enzymes produced by large scale only cost around several hundred euros per kilogram was recorded. If considered an estimated average price for free P450 BM3 enzyme to be around US$ 100 kg^{-1}, new nanobiocatalyst will have an additional advantage in terms of operating cost, being 5 times lower than those values obtained when free P450 BM3 enzyme is used (US$ 100 kg^{-1}). Moreover, free P450 BM3 enzyme depends on a coenzyme as an electron source, namely nicotinamide adenine dinucleotide (NADH) or its phosphorylated form (NADPH) that are consumed during reaction. The high cost of NAD (P) H (bulk price per mol: $3000 for NADH and $215,000 for NADPH) (~1300 USD/g) [61]. Hydrogen peroxide (H_2O_2) was used instead of NADPH in the new nanobiocatalyst. Comparing the lower cost of H_2O_2 cofactor ($0.0004 price per gram) used in the new system; which is 300 times lower than NADPH price to drive electron transfer in the P450 catalysis significantly affects the cost of the scale-up of the biocatalytic process. For the evaluation of the economic process, it's clear that both the amount of enzyme used and the cost of the cofactors had a great impact of the final product cost. Thus, the low cost of novel nanbiocatalyst is likely to become a strong catalyst candidate for VOCs removal in this study and other industrial applications as drugs, hydrocarbons, xenobiotics, fatty acids, and aromatic compounds for further investigation.

4. Conclusions

The cytochrome P450 BM3 enzyme produced by engineered *E. coli* was immobilized by adsorption and cross-linking-adsorption on Pt/TiO_2-Cu hollow nanosphere to create an effective novel bionanocatalyst that can be significantly used for organic pollutants degradation under visible light conditions for the first time. The hollow nano-composite TiO_2–Cu enhances the stability and activity of immobilized P450 BM3 enzyme over the free enzyme. Moreover, a combination of nanomaterial and enzyme is required for achieving biocompatibility and inert condition without denaturing the enzyme. This approach has two benefits: The first benefit is the introduction of a technology designed to stabilize the enzyme on a solid substrate. This resolves the problem of weak enzyme stability, low operational stability, and short shelf life during long-term storage and reuse, which are a major issue and one of the biggest restrictions in the use of pure enzymes in various industrial applications. The second benefit is the augmentation of the catalytic performance of the enzyme via synergetic combination of the biocatalytic property of the enzyme and photocatalytic property of the hollow nanosphere Pt-TiO_2–Cu composite due to the presence of Pt and TiO_2 photo-characteristics. In addition, the hollow nanoparticle generates a pair of electron-hole pairs under solar radiation. Thus, the hollow nanoparticle helped to produce continuous supply of electrons to the enzyme instead of using expensive nicotinamide adenosine dichlorocyclide phosphate (NADPH) and thus with this economic low cost it could be widely used in the industry. Briefly, the main objective of this study is to provide an environmentally friendly hollow nanostructured biocatalyst, and this system represents a possible and effective approach to control environmental pollution with a bright future in various industrial, pharmaceutical and environmental applications as a new photonanobiocatalyst using the visible spectrum of sunlight.

Disclosure statement

No potential conflict of interest was reported by the authors.

Acknowledgments

Funding and laboratory facilities were provided by the Air Pollution Department and Chemistry of Natural and Microbial Products Department of the National Research Centre, Egypt that are gratefully acknowledged.

References

[1] S. Salvador, J.M. Commandre, Y. Kara, Thermal recuperative incineration of VOCs: CFD modelling and experimental validation, Appl. Therm. Eng. 26 (2006) 2355–2366.
[2] J. Palau, J.M. Penya-Roja, C. Gabaldon, F.J. Alvarez-Hornos, V. Martinez-Soria, Effect of pre-treatments based on UV photocatalysis and photo-oxidation on toluene biofiltration performance, J. Chem. Technol. Biot. 87 (2012) 65–72.
[3] C. Andriantsiferana, E.F. Mohamed, H. Delmas, Sequential adsorption - photocatalytic oxidation process for wastewater treatment using a composite material TiO_2/activated carbon, Environ. Eng. Res. 20 (2015) 181–189.
[4] E.F. Mohamed, M.A. El-Hashemy, N.M. Abdel-Latif, Production of sugarcane bagasse-based activated carbon for formaldehyde gas removal from potted plants exposure chamber, J. Air Waste Manage. Assoc. 65 (2015) 1413–1420.
[5] H. Zaitan, E.F. Mohamed, H. Valdés, M. Nawdali, S. Rafqah, M.H. Manero, Toluene, Methanol and Benzaldehyde Removal from Gas Streams by Adsorption onto Natural Clay and Faujasite-Y type Zeolite, Acta Chim. Slov. 63 (2016) 798–808.
[6] Y. Zhang, J. Moa, Y. Li, J. Sundell, P. Wargocki, J. Zhang, et al., Can commonly-used fan-driven air cleaning technologies improve indoor air quality? A literature review, Atmos. Environ. 45 (2011) 4329–4343.
[7] D. Vildozo, R. Portela, C. Ferronato, J.M. Chovelon, Photocatalytic oxidation of 2-propanol/toluene binary mixtures at indoor air concentration levels, Appl. Catal. B 107 (2011) 347–354.
[8] W. Zhao, Y. Yang, J. Dai, F. Liu, Y. Wang, VUV photolysis of naphthalene in indoor air: intermediates, pathways, and health risk, Chemosphere 91 (2013) 1002–1008.
[9] C. Andriantsiferana, E.F. Mohamed, H. Delmas, Photocatalytic degradation of an azo-dye on TiO_2 activated carbon composite material, Environ. Technol. 35 (2013) 355–363.
[10] H. Essawy, A. Shakour, M. Tawfik, E.F. Mohamed, S. El-Sabbagh, M. El-Hashemy,

Composite membranes derived from immiscible NBR/SBR blends and amphiphilic montmorillonites: permeability evaluation of these membranes for benzene and toluene in their binary mixtures, RSC Adv. 4 (2014) 33555–33563.
[11] E.F. Mohamed, S.A. Sayed Ahmed, N.M. Abdel-Latif, A. ELMekawy, Air purifier devices based on adsorbents produced from valorization of different environmental hazardous materials for ammonia gas, RSC Adv. 6 (2016) 57284–57292.
[12] E.F. Mohamed, G. Awad, H. Zaitan, C. Andriantsiferana, M.-H. Manero, Transition metals-incorporated zeolites as environmental catalysts for indoor air ozone decomposition, Environ. Technol. 39 (2018) 878–886.
[13] E.F. Mohamed, G. Awad, C. Andriantsiferana, A.I. El-Diwany, Biofiltration technology for the removal of toluene from polluted air using Streptomyces griseus, Environ. Technol. 37 (2016) 1197–1207.
[14] S. Malakar, P. Das Saha, D. Baskaran, R. Rajamanickam, Microbial biofilter for toluene removal: performance evaluation, transient operation and theoretical prediction of elimination capacity, Sustainable Environ. Res. 28 (2018) 121–127.
[15] Q. Husain, Peroxidase mediated decolorization and remediation of wastewater containing industrial dyes: a review, Rev. Environ. Sci. Biotechnol. 9 (2010) 117–140.
[16] N. Coconi-Linares, E. Ortiz-Vázquez, F. Fernández, A.M. Loske, M.A. Gómez-Lim, Recombinant expression of four oxidoreductases in Phanerochaete chrysosporium improves degradation of phenolic and non-phenolic substrates, J. Biotechnol. 209 (2015) 76–84.
[17] J. Li, J. Peng, Y. Zhang, Y. Ji, H. Shi, L. Mao, S. Gao, Removal of triclosan via peroxidases-mediated reactions in water: reaction kinetics, products and detoxification, J. Hazard. Mater. 310 (2016) 152–160.
[18] A.H. Alneyadi, S.S. Ashraf, Differential enzymatic degradation of thiazole pollutants by two different peroxidases—a comparative study, Chem. Eng. J. 303 (2016) 529–538.
[19] M. Bilal, M. Asgher, H.M. Iqbal, H. Hu, X. Zhang, Bio-based degradation of emerging endocrine-disrupting and dye-based pollutants using cross-linked enzyme aggregates, Environ, Sci. Pollut. Res. 24 (2017) 7035–7041.
[20] S.B. Bankar, M.V. Bule, R.S. Singhal, L. Ananthanarayan, Glucose oxidase, An overview, Biotechnol. Adv. 27 (2009) 489–501.
[21] M.-A. Constantin, J. Conrad, U. Beifuss, Laccase-catalyzed oxidative phenolic coupling of vanillidene derivatives, Green Chem. 14 (2012) 2375–2379.
[22] J.-M. Choi, S.-S. Han, H.-S. Kim, Industrial applications of enzyme biocatalysis: current status and future aspects, Biotechnol. Adv. 33 (2015) 1443–1454.
[23] A. Madhavan, R. Sindhu, P. Binod, R.K. Sukumaran, A. Pandey, Strategies for design of improved biocatalysts for industrial applications, Bioresour. Technol. 245 (2017) 1304–1313.
[24] I. Roy, S. Prasad, Converting enzymes into tools of industrial importance, Recent Pat. Biotechnol. 12 (2017) 33–56.
[25] S. Li, X. Yang, S. Yang, M. Zhu, X. Wang, Technology prospecting on enzymes: application, marketing and engineering, Comput. Struct. Biotechnol. J. 9 (2012) 11.
[26] X. Li, H. Zhu, J. Feng, J. Zhang, X. Deng, B. Zhou, H. Zhang, D. Xue, F. Li, N.J. Mellors, et al., One-pot polylol synthesis of graphene decorated with size- and density-tunable Fe_3O_4 nanoparticles for porcine pancreatic lipase immobilization, Carbon 60 (2013) 488–497.
[27] C. Li, S. Jiang, X. Zhao, H. Liang, Co-Immobilization of Enzymes and Magnetic Nanoparticles by Metal-Nucleotide Hydrogelnanofibers for Improving Stability and Recycling, Molecules 22 (2017) 1–11.
[28] J. Mehta, N. Bhardwaj, S.K. Bhardwaj, K.-H. Kim, A. Deep, Recent advances in enzyme immobilization techniques: metal-organic frameworks as novel substrates, Coord. Chem. Rev. 322 (2016) 30–40.
[29] A.G. Grigoras, Catalase immobilization—a review, Biochem. Eng. J. 117 (2017) 1–20.
[30] J. Chapman, A.E. Ismail, C.Z. Dinu, Industrial applications of enzymes: recent advances, techniques, and outlooks, Catalysts 8 (2018) 1–26.
[31] C.S. Bezerra, C.M.G.D.F. Lemos, M.D. Sousa, L.R.B. Goncalves, Enzyme immobilization onto renewable polymeric matrixes: past, present and future trends, J. Appl. Polym. Sci. 132 (2015) 1–15.
[32] C. Cai, Y. Gao, Y. Liu, N. Zhong, N. Liu, Immobilization of *Candida antarctica* lipase B onto SBA-15 and their application in glycerolysis for diacylglycerols synthesis, Food Chem. 212 (2016) 205–212.
[33] Y. Liu, H. Zhou, L. Wang, S. Wang, Stability and catalytic properties of lipase immobilized on chitosan encapsulatedmagnetic nanoparticles cross-linked with genipin and glutaraldehyde, J. Chem. Technol. Biotechnol. 91 (2016) 1359–1367.
[34] N.L.D. Nyari, I.A. Fernandes, C.E. Bustamante-Vargas, C. Steffens, D. de Oliveira, J. Zeni, E. Rigo, R.M. Dallago, In situ immobilization of *Candida antarctica* B lipase in polyurethane foam support, J. Mol. Catal. B Enzym. 124 (2016) 52–61.
[35] S.A. Ansari, Q. Husain, Potential applications of enzymes immobilized on/in nano materials: a review, Biotechnol. Adv. 30 (2012) 512–523.
[36] U. Guzik, K. Hupert-Kocurek, M. Krysiak, D. Wojcieszyńska, Degradation potential of protocatechuate 3,4-dioxygenase from crude extract of *Stenotrophomonas maltophilia* strain KB2 immobilized in calcium alginate hydrogels and on glyoxy agarose, Biomed Res. Int. 138768 (8) (2014) 1–138768.
[37] P. Esmaeilnejad-Ahranjani, M. Kazemeini, G. Singh, A. Arpanaei, Amine-functionalized magnetic nanocomposite particles for efficient immobilization of lipase: effects of functional molecule size on properties of the immobilized lipase, RSC Adv. 5 (2015) 33313–33327.
[38] S. Cao, P. Xu, Y. Ma, X. Yao, Y. Yao, M. Zong, X. Li, W. Lou, Recent advances in immobilized enzymes on nanocarriers, Chin. J. Catal. 37 (2016) 1814–1823.
[39] F. Tian, Y. Guo, F. Lin, Y. Zhang, Q. Yuan, H. Liang, Rational surface silane modification for immobilizing glucose oxidase, Int. J. Biol. Macromol. 87 (2016) 191–194.
[40] C.C. Nguyen, N.N. Vu, Trong-On Do, Recent advances in the development of sunlight-driven hollow structure photocatalysts and their applications, J. Mater. Chem. A (3) (2015) 18345–18359.
[41] B. Viswanath, B. Rajesh, A. Janardhan, A.P. Kumar, G. Narasimha, Fungal laccases and their applications in bioremediation, Enzyme Res. (2014) (2014) 163242.
[42] G.K. Hupert-Kocurek, D. Wojcieszyńska, Immobilization as a strategy for improving enzyme properties-application to oxidoreductases, Urszula Molecules 19 (2014) 8995–9018.
[43] N. Patel, S. Shahane, S. Shivam, R. Majumdar, U. Mishra, Mode of action, properties, production, and Application of Laccase: A Review (2018), https://doi.org/10.2174/1872208312666180821161015.
[44] C.J. Whitehouse, S.G. Bell, L.L. Wong, P450 (BM3) (CYP102A1): connecting the dots, Chem. Soc. Rev. 41 (2012) 1218–1260.
[45] A. Bahrami, T. Vincent, A. Garnier, F. Larachi, J. Boukouvalas, M.C. Iliuta, Noncovalent immobilization of optimized bacterial cytochrome P450 BM3 on functionalized magnetic nanoparticles, Ind. Eng. Chem. Res. 56 (2017) 10981–10989.
[46] D.J. King, M.R. Azari, A. Wiseman, Immobilization of a Cytochrome P-450 Enzyme from Saccharomyces Cerevisiae, Methods, Enzymol. 137 Academic Press, 1988, pp. 675–686.
[47] T. Omura, R. Sato, The carbon monoxide-binding pigment of liver microsomes: I evidence for its hemoprotein nature, J. Biol. Chem. 239 (1964) 2370–2378.
[48] F.P. Guengerich, M.V. Martin, C.D. Sohl, Q. Cheng, Measurement of cytochrome P450 and NADPH–cytochrome P450 reductase, Nat. Protoc. 4 (2009) 1245–1251.
[49] D. Türkmen, H. Yavuz, A. Denizli, Synthesis of tentacle type magnetic beads as immobilized metal chelate affinity support for cytochrome c adsorption, Int. J. Biol. Macromol. 38 (2006) 126–133.
[50] S.F. Motevalizadeh, M. Khoobi, A. Sadighi, M. KhalilvandSedagheh, M. Pazhouhandeh, A. Ramazani, M.A. Faramarzi, A. Shafiee, Lipase immobilization onto polyethylenimine coated magnetic nanoparticles assisted by divalent metal chelated ions, J. Mol. Catal., B Enzym. 120 (2015) 75–83.
[51] L. Cao, Adsorption-based immobilization, Carrier-bound Immobilized Enzymes, Wiley-VCH Verlag GmbH & Co. KG KGaA, Weinheim, Germany, 2006, pp. 53–168.
[52] T.T. Xia, C.Z. Liu, J.H. Hu, C. Guo, Improved performance of immobilized laccase on amine-functioned magnetic Fe_3O_4 nanoparticles modified with polyethylenimine, Chem. Eng. J. 295 (2016) 201–206.
[53] E. Dehghanifard, A. Jafari, R. Kalantary, A. Mahvi, M. Faramarzi, A. Esrafili, Biodegradation of 2,4-dinitrophenol with laccase immobilized on nano-porous silica beads, Iranian J. Environ. Health Sci. Eng. 10 (2013) 2–9.
[54] B.Y.H. James, Behrendorff, M.J. Elizabeth, Gillam, Prospects for applying synthetic biology to toxicology: future opportunities and current limitations for the repurposing of cytochrome P450 systems, Chem. Res. Toxicol. 30 (2017) 453–468.
[55] R. Ahmad, M. Sardar, Enzyme immobilization: an overview on nanoparticles as immobilization matrix, Biochem. Anal. Biochem. 4 (2015) 178.
[56] G. Li, A.G. Nandgaonkar, Q. Wang, J. Zhang, W.E. Krause, Q. Wei, L.A. Lucia, Laccase-immobilized bacterial cellulose/TiO2 functionalized composite membranes: evaluation for photo- and bio-catalytic dye degradation, J. Membrane Sci. 525 (2017) 89–98.
[57] J. Lin, L. Fan, R. Miao, X. Le, S. Chen, X. Zhou, Enhancing catalytic performance of laccase via immobilization on chitosan/CeO_2 microspheres, Int. J. Biol. Macromol. 78 (2015) 1–8.
[58] E.P. Cipolatti, A. Valerio, R.O. Henriques, D.E. Moritz, J.L. Ninow, D.M.G. Freire, E.A. Manoel, R. Fernandez-Lafuente, D.D. Oliveira, Nanomaterials for biocatalyst immobilization—state of the art and future trends, RSC Adv. 6 (2016) 104675–104692.
[59] R.A. Sheldon, S. van Pelt, Enzyme immobilization in biocatalysis: why, what and how, Chem. Soc. Rev. 42 (2013) 6223–6235.
[60] J.J. Dong, E. Fernández-Fueyo, F. Hollmann, C.E. Paul, M. Pesic, S. Schmidt, Y. Wang, S. Younes, W. Zhang, Biocatalytic oxidation reactions: a chemist's perspective, Angew. Chem. Int. Ed. Engl. 57 (2018) 9238–9261.
[61] X. Wang, T. Saba, H.H.P. Yiu, R.F. Howe, J.A. Anderson, J. Shi, Cofactor NAD(P)H regeneration inspired by heterogeneous pathways, Chem 2 (2017) 621–654.